Thioredoxin Reductase from *Thermoplasma acidophilum*: A New Twist on Redox Regulation[†,‡]

Hector H. Hernandez,[§] Orlando A. Jaquez,[||] Michael J. Hamill,[⊥] Sean J. Elliott,[⊥] and Catherine L. Drennan*[,§,||]

Departments of Chemistry and Biology, Massachusetts Institute of Technology, 16-573, 77 Massachusetts Avenue, Cambridge, Massachusetts 02139, and Department of Chemistry, Boston University, 590 Commonwealth Avenue, Boston, Massachusetts 02215

Received April 16, 2008; Revised Manuscript Received July 11, 2008

ABSTRACT: Thioredoxin reductases (TrxRs) regulate the intracellular redox environment by using NADPH to provide reducing equivalents for thioredoxins (Trxs). Here we present the cloning and biochemical characterization of a putative TrxR (Ta0984) and a putative Trx (Ta0866) from *Thermoplasma acidophilum*. Our data identify Ta0866 as a Trx through its capacity to reduce insulin and be reduced by *Escherichia coli* TrxR in a NADPH-dependent manner. Our data also establish Ta0984 as a TrxR due to its ability to reduce *T. acidophilum* Trx (*ta*Trx), although not in a NADPH- or NADH-dependent manner. To explore the apparent inability of *ta*TrxR to use NADPH or NADH as a reductant, we carried out a complete electrochemical characterization, which suggests that redox potential is not the source of this nonreactivity [Hamill et al. (2008) *Biochemistry 47*, 9738−9746]. Turning to crystallographic analysis, a 2.35 Å resolution structure of *ta*TrxR, also presented here, shows that despite the overall structural similarity to the well-characterized TrxR from *E. coli* (RMSD 1.30 Å^2 for chain A), the "NADPH binding pocket" is not conserved. *E. coli* TrxR residues implicated in NADPH binding, H175, R176, R177, and R181, have been substituted with E185, Y186, M187, and M191 in the *ta* protein. Thus, we have identified a Trx and TrxR protein system from *T. acidophilum* for which the TrxR shares overall structural and redox properties with other TrxRs but lacks the appropriate binding motif to use the standard NADPH reductant. Our discovery of a TrxR that does not use NADPH provides a new twist in redox regulation.

Tight regulation of the cellular redox environment is crucial for cell survival. Cellular viability relies on the reduction of metabolites for energy production, on the oxidation of small molecules to assemble structural scaffolds, and on the maintenance of the proper disulfide state in the extracellular or intracellular environments. An imbalance in redox regulation can trigger a cascade of genetic responses, the most extreme of which can lead to cell death (reviewed in refs *1*−*4*).

The principal protein systems that act as reductants are NADPH[1]-dependent thioredoxin reductase (TrxR)/thioredoxin (Trx) and glutathione reductase (GSSGR)/glutathione (GDH)/glutaredoxin (Grx) (Figure 1A) (*1, 2, 4*−*6*). NADPH reduces the FAD of TrxRs, which in turn reduces Trxs through disulfide exchange (Figure 1B). The TrxR/Trx system is responsible for providing reducing equivalents for many cellular processes including the reduction of ribonucleotide reductase (RNR) during the conversion of nucleotides to deoxynucleotides (*7*). This reaction is essential for maintaining the appropriate levels of deoxynucleotides in the cell for DNA repair and for cellular replication (*8, 9*). The significance of the redox regulation of these and other biochemical pathways has led to renewed interest in antibacterial or antitumorgenic therapies that are targeted to disrupt redox regulation (*1, 10*−*13*).

Here we study putative TrxR and Trx from *Thermoplasma acidophilum*, an organism first isolated from a self-heating coal refuse pile at the Friar Tuck mine in southwest Indiana. This organism lacks a cell wall, and optimal growth occurs at 59 °C and at pH 1−2 (*14*). Despite the organism's ability to grow at low pH, the cytoplasmic pH of *T. acidophilum* was reported to be between 5.5 and 6.9 (*15, 16*). The 1.56 Mb genomic sequence of *T. acidophilum* encoding 1509 open reading frames (ORFs) has been reported (*17*), allowing us to identify a putative TrxR (Ta0984) and Trx (Ta0866).

[†] This work was supported by NIGMS Ruth L. Kirschstein predoctoral fellowship GM73569 (H.H.H.), National Institutes of Health Grant GM65337 (C.L.D.), and the Richard Allan Barry Fund of the Boston Foundation (S.J.E.).

[‡] The atomic coordinates and structure factor amplitudes have been deposited in the Protein Data Bank (www.rcsb.org) as entry 3CTY.

* To whom correspondence should be addressed. Phone: (617) 253-5622. Fax: (617) 258-7847. E-mail: cdrennan@mit.edu.

[§] Department of Chemistry, Massachusetts Institute of Technology.

[||] Department of Biology, Massachusetts Institute of Technology.

[⊥] Department of Chemistry, Boston University.

[1] Abbreviations: Trx, thioredoxin; TrxR, thioredoxin reductase; Grx, glutaredoxin; GDH, glutathione; GSSGR, glutathione reductase; RNR, ribonucleotide reductase; ORF, open reading frame; Tris-HCl, tris(hydroxymethyl)aminomethane hydrochloride; PMSF, phenylmethanesulfonyl fluoride; PCR, polymerase chain reaction; DTT, 1,4-dithio-DL-threitol; HEPES, *N*-(2-hydroxyethyl)piperazine-*N*′-2-ethanesulfonic acid; *ec*, *Escherichia coli*; EDTA, ethylenediaminetetraacetic acid; FAD, flavin adenine dinucleotide; $FADH_2$, flavin adenine dinucleotide, reduced form; FO, flavin oxidizing conformation; FR, flavin reducing conformation; NADH, nicotinamide adenine dinucleotide, reduced form; NADPH, nicotinamide adenine dinucleotide phosphate, reduced form; SafO, safranine O; *ta*, *Thermoplasma acidophilum*; XO, xanthine oxidase.

10.1021/bi8006753 CCC: $40.75 © 2008 American Chemical Society
Published on Web 08/22/2008

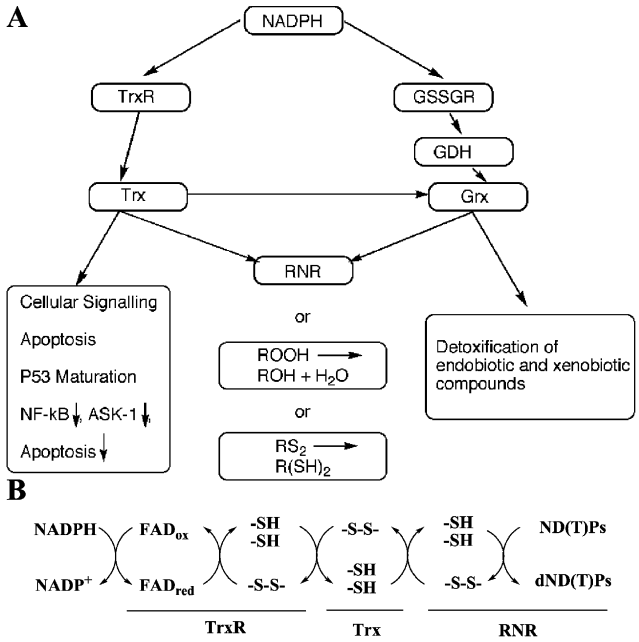

FIGURE 1: NADPH participation in cellular redox regulation. (A) NADPH-dependent redox regulatory pathways. (B) A mechanism of NADPH-dependent cellular reduction by the thioredoxin reductase system.

We report the cloning, expression, and purification of gene products Ta0984 and Ta0866 and show that Ta0866 exhibits thioredoxin-like activity and that Ta0984 is able to reduce *T. acidophilum* Trx (*ta*Trx), establishing its identity as a thioredoxin reductase. An accompanying paper (*46*) describes the full electrochemical characterization of *T. acidophilum* TrxR (*ta*TrxR). While the redox potential is within the expected range for TrxRs, we find that the standard TrxR reducing agents NADPH and NADH do not reduce the *ta*TrxR flavin. The X-ray structure of *ta*TrxR to 2.35 Å resolution presented here reveals a major modification of the classic TrxR NADPH binding site, suggesting that *T. acidophilum* may utilize a novel reductant.

EXPERIMENTAL PROCEDURES

Materials. The organism *T. acidophilum* (ATCC number 27656) was obtained from the American Tissue Culture Center. TOPO and TOPO Zero Blunt PCR cloning kits were obtained from Invitrogen (Carlsbad, CA). NovaBlue competent cells, Rosetta (DE3)pLysS competent cells, and pET28a plasmid were purchased from Novagen (Madison, WI). *pfu*Turbo DNA polymerase and a PCR optimization kit were obtained from Stratagene (Cedar Creek, TX). Primers were obtained from Integrated DNA Technologies (Coralville, IA). Nickel nitrilotriacetic acid (Ni-NTA) was purchased from Qiagen (Valencia, CA). Restriction enzymes were purchased from New England BioLabs (Beverly, MA). Kanamycin, chloramphenicol, Tris-HCl, ethylenediaminetetraacetic acid (EDTA), and phenylmethanesulfonyl fluoride (PMSF) were obtained from Sigma-Aldrich (St. Louis, MO).

Genomic Analysis of T. acidophilum Genome. The genome of *T. acidophilum DSM1728* (RefSeq NC_002578, GenBank AL139299) was analyzed using the web interface at the National Center for Biotechnology Information (http://www.ncbi.nlm.nih.gov) for putative thioredoxin reductase (TrxR) and thioredoxin (Trx) open reading frames (ORFs). An ORF encoding a 319 amino acid protein, Ta0984, and an ORF encoding for a 113 amino acid protein, Ta0866, were identified by sequence homology to known TrxRs and Trxs using PSI-BLAST (*18*). Protein sequences were aligned using the program ClustalW (*19*), and the output was rendered using the web interface ESPript 2.2 (*20*) (Supporting Information Figure S1 and S2).

Cloning of taTrxR and taTrx. The *ta*TrxR and *ta*Trx genes were amplified by the polymerase chain reaction (PCR) using genomic DNA from a cell suspension and the primers 5′-A TGC CAT ATG GCA TAT GGA ATT TAA CCT GCA TGC AGT A-3′ and 5′-TCA GCC AAG CTT CAT TTT TTG GAT ATA GAA TCA-3′ for *ta*TrxR and 5′-A TGC CAT ATG GCA TAT GAA GAA TTA TAT GGG CTG CG-3′ and 5′-TAG CGG CCG CTC AGA CGG AAT CGC AGG GA-3′ for *ta*Trx (restriction sites are underlined). PCR products were cloned into the expression vector pET28a using *Nde*I and *Hin*dIII restriction enzymes for *ta*TrxR and *Nde*I and *Not*I for *ta*Trx. The sequence of the pET28a-taTrxR and pET28a-taTrx cDNA was confirmed at the MIT Biopolymers Sequencing Facility (Supporting Information Figures S3 and S4). After confirmation of the correct sequences, the resulting constructs were transformed into Rosetta (DE3)pLysS cells for facile protein expression.

Purification of Recombinant taTrxR and taTrx. Rosetta (DE3)pLysS transformed with either pET28a-taTrxR or pET28a-taTrx constructs were used to inoculate TB media supplemented with 20 μg mL^{-1} kanamycin and 34 μg mL^{-1} chloramphenicol. The culture was grown at 37 °C to an OD_{600} of 0.8 and induced with 0.8 mM isopropyl thio-β-D-galactoside (IPTG) for 4 h. The cells were harvested by centrifugation, resuspended in lysis buffer (10 mM Tris-HCl, pH 8.0, 150 mM NaCl, 10 mM imidazole, 1 mM PMSF), and disrupted by sonication using a Digital Sonifier 250 (Branson, CN). Insoluble material was removed by ultracentrifugation at 40000*g* using a Beckman Avanti J-25 centrifuge (Beckman, PA, CA). The supernatant was subjected to heating at 70 °C for 45 min and then centrifuged at 40000*g*. The clarified supernatant was loaded onto a Ni-NTA column, washed with high salt buffer, and eluted with buffer containing 10 mM Tris-HCl, pH 8.0, 150 mM NaCl, and 200 mM imidazole. Eluted fractions were analyzed by a SDS−PAGE 4−20% gel, and those fractions containing proteins with comparable size to *ta*TrxR or *ta*Trx were concentrated using an Amicon (Millipore, Bedford, MA) stirred ultrafiltration cell.

The eluted protein was dialyzed overnight in 20 mM HEPES, pH 7.5, 20 mM NaCl, 0.5 mM EDTA, and 1 mM 1,4-dithio-DL-threitol (DTT) with thrombin (0.05 unit mL^{-1}) to remove the N-terminal poly-His tag. The digested protein fraction was loaded onto an SEC-30 high-prep size exclusion column from Amersham Biosciences (Piscataway, NJ), which was preequilibrated with storage buffer (10 mM HEPES, pH 7.0, 20 mM NaCl). Fractions containing protein of either MW ~34 kDa (*ta*TrxR) or MW ~13 kDa (*ta*Trx) were concentrated using a Centriprep YM-3 filter from Amicon (Millipore, Bedford, MA). Protein purity was analyzed by SDS−PAGE 4−20% gel (Supporting Information Figure S5), and protein concentration was determined from the theoretical extinction coefficient at 280 nm (23040 M^{-1} cm^{-1} for *ta*TrxR and 16500 M^{-1} cm^{-1} for *ta*Trx) (ProtParam, ExPaSy web server). A Cary 300 spectrophotometer (Varian,

Table 1: Data and Refinement Statistics for *ta*TrxR Structure

	native
Data Set	
wavelength (Å)	1.2710
beamline	ALS 5.0.2
space group	*I*23
$a = b = c$ (Å)	165.95
resolution (Å)	50−2.35
R_{sym} (%)	6.9 (52.1)[a]
no. of observations	434549
unique observation	31586
$I/\sigma I$	32.9 (7.6)
completeness (%)	99.9 (100.0)
Refinement Statistics	
resolution limits (Å)	50−2.35
no. of reflections	31128
no. of reflections (test set)	1809
R_{work} (%)[b]	22.5
R_{free} (%)[c]	26.0
Wilson *B* factor (Å^2)	68.3
B factor chain A (Å^2)	55.4
B factor chain B (Å^2)	62.1
B factor FAD 1 (Å^2)	49.2
B factor FAD 2 (Å^2)	59.4
B factor waters (Å^2)	68.0
solvent content (%)	56.4
no. of protein atoms	2272 (2285)[d]
no. of water atoms	111
no. of nonprotein atoms (FAD)	106
bond length deviation (Å)	0.0073
bond angle deviation (deg)	1.2
Ramachandran Plot	
residues in most favored regions (%)	93.6
residues in allowed region (%)	6.2
residues in disallowed region (%)	0.2

[a] Statistics for highest resolution shell (2.35−2.43 Å) are in parentheses. [b] $R_{work} = \sum||F_o| - |F_c||/\sum|F_o|$. [c] R_{free} calculated using 5% of the total reflections, which were not used in refinement. [d] Number of atoms in chain A and chain B.

CA) was used to analyze the purified *ta*TrxR for flavin incorporation.

Temperature Stability of NADPH and NADH. NADPH (0.22 μM) and NADH (0.26 μM) were analyzed for temperature-dependent degradation in 50 mM Tris-HCl, pH 7.5, and 150 mM NaCl (Figure S6). Initial UV/visible spectra were collected at 20 °C from 800 to 240 nm. The temperature was increased to 80 °C, and the reaction was allowed to equilibrate for 5 min before full spectra were collected. The reaction was cooled to 20 °C, and then another full spectrum was collected. To measure time-dependent degradation, NADPH or NADH was heated to the desired temperature (20, 60, and 80 °C), and a reading was collected at 340 nm in 5 min increments for 45 min. Degradation of NADPH or NADH was inferred from the decrease in absorbance at 340 nm normalized to 100% of the absorbance for the sample at time zero. Experiments were performed in triplicate.

Activity of taTrx Measured by Insulin and DTT Assays. Purified *ta*Trx was assayed for disulfide reductase activity by the insulin reduction method (*21*). The standard assay mixture contained 1.25 mM bovine insulin, 100 mM potassium phosphate, pH 7.0, 2 mM EDTA, and *ta*Trx (43, 66, or 70 μM). The reaction was initiated by the addition of 1 mM DTT. An increase in absorbance at 650 nm was monitored at 25 °C.

Purified oxidized *ta*Trx was also assayed for its ability to be reduced by *ec*TrxR using the DTNB method (*22*). Briefly, this colorimetric assay measures the Trx-dependent reduction of DTNB to 5-thio-2-nitrobenzoic acid (TNB), which absorbs strongly at 405−414 nm, using TrxR and NADPH as electron donors. The reaction was performed using 3.8 μM *ec*TrxR, in 50 mM Tris-HCl, pH 8.0, 2 mM EDTA, 0.5 mM NADPH, and 0.6 mM DTNB. Each assay was initiated by the addition of *ta*Trx (5−60 μM) to the reaction mixture, and the conversion of DTNB to TNB was monitored by the increase in absorbance at 412 nm.

Titration of taTrxR and ecTrxR with NADPH and NADH. *ta*TrxR (43.3 μM) was titrated with NADPH or with NADH (0.5−5.0 mol of NAD(P)H/mol of FAD) under anaerobic conditions at 59 °C in 50 mM Tris-HCl, pH 7.5, and 150 mM NaCl. Spectra were collected from 800 to 240 nm to monitor the reduction of the enzyme-bound flavin by NADPH or NADH. *ec*TrxR (40.5 μM) was titrated with NADPH or with NADH (0.5−5.0 mol of NADPH or NADH/mol of FAD) under anaerobic conditions at 25 °C in 50 mM Tris-HCl, pH 7.5, and 150 mM NaCl. Spectra for NADPH reduction of *ec*TrxR were recorded as described above and were corrected for dilution. The reduction of bound FAD was monitored by observing the change in absorbance at 457 nm over 45 min. *ta*TrxR (43.3 μM) and *ec*TrxR (40.5 μM) were titrated with 2.5 mM NADPH or NADH for 45 min. For *ta*TrxR, spectra were collected every minute, and for *ec*TrxR, spectra were collected every 0.1 min for the initial 5 min and then every 5 min thereafter.

Ability of taTrxR To Reduce taTrx. To verify that the reduced *ta*TrxR was capable of passing electrons to *ta*Trx, the xanthine/xanthine oxidase reduction system, described by Massey and co-workers, was used (*23*). After complete reduction of a sample of *ta*TrxR, the reoxidation of *ta*TrxR (4 μM) was monitored spectroscopically in the visible region following the addition of *ta*Trx or *ec*Trx (8 μM). In a 1 cm path length curvette stirred continuously and held at 25 °C in a MBraun Labmaster glovebox, the *ta*TrxR reduction was performed as follows: to a solution of 100 mM phosphate buffer (pH 7.5) with 1 μM benzyl viologen, 250 μ xanthine, and 4 μM *ta*TrxR, an aliquot of xanthinc oxidase was added to a final concentration of ~0.25 nM to initiate the reaction. This solution was monitored in the visible region of the spectrum, using an SI Photonics spectrophotometer contained within the glovebox, over the course of 1.5 h, upon which complete reduction of the *ta*TrxR was achieved. Oxidized Trx was then added to a final concentration of 8 μM, and the spectral features were monitored.

Analysis of T. acidophilum Genome for Alternative Redox Regulation Pathways. To investigate if *T. acidophilum* uses alternative characterized reduction pathways, the *T. acidophilum* genome was mined for known pathways using NCBI BLAST (*18*) to compare known proteins involved in the formation of glutathione or of coenzyme F420 to the ORFs of *T. acidophilum*. Pathway members were identified using ExPASy PATHWAY service (http://ca.expasy.org/cgi-bin/lists?pathway.txt).

Crystallization and Data Collection. *ta*TrxR was crystallized by incubating 2.0 μL of protein solution (65 mg mL^{-1} *ta*TrxR in 10 mM HEPES, pH 7.5, and 20 mM NaCl) and 2.0 μL of precipitant solution (0.28 M $MgCl_2$, 0.1 M Bis-Tris, pH 5.5, 25% (w/v) PEG 3350) in a sitting drop at room temperature. Crystals had cubic geometry, and their bright yellow color confirmed the incorporation of FAD by the enzyme. They grew to approximately 100 μM per side in

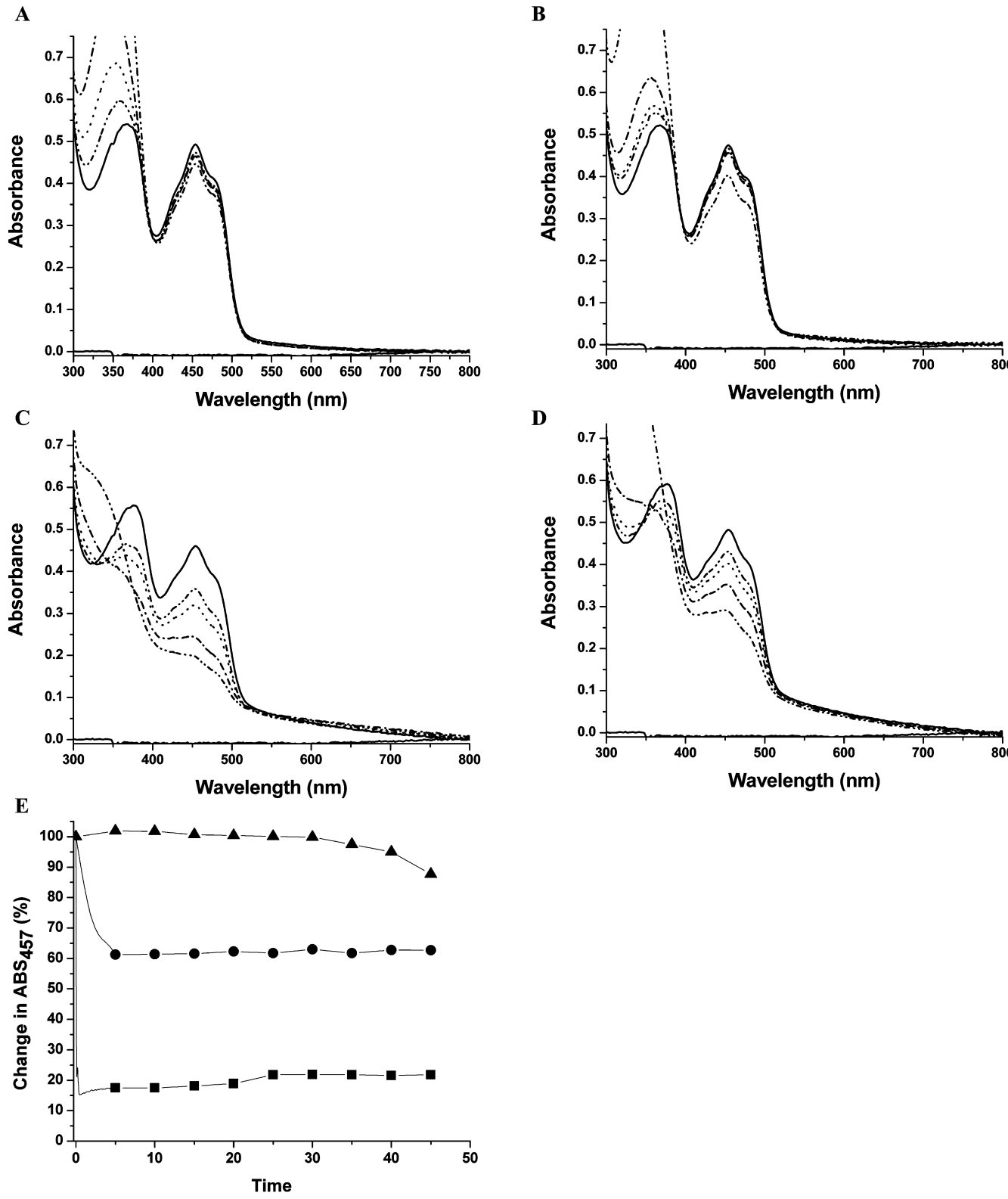

FIGURE 2: Anaerobic titration of *ta*TrxR and *ec*TrxR with NADPH and NADH. (A) Visible spectra of *ta*TrxR (43.3 μM) titrated with NADPH at 59 °C. Solid line is without NADPH, dashed line is with 0.5 mol of NADPH/mol of FAD, dotted line is with 1.0 mol of NADPH, dash-dot line is with 2.0 mol of NADPH, and dash-dot-dot line is with 5 mol of NADPH. (B) Visible spectra of *ta*TrxR titrated with NADH at 59 °C. (C) Visible spectra of *ec*TrxR (40.5 μM) titrated with NADPH at 25 °C. (D) Visible spectra of *ec*TrxR (40.5 μM) titrated with NADH at 25 °C. Spectra B−D were recorded as in spectrum A. (E) Time-dependent reduction of *ta*TrxR and NADPH at 59 °C (closed triangles), *ta*TrxR and NADH at 59 °C (closed circles), and *ec*TrxR at 25 °C with NADPH (closed squares).

3−4 days. These crystals were soaked for 30 s in a cryoprotectant solution of 0.28 M $MgCl_2$, 0.1 M Bis-Tris, pH 5.5, 25% (w/v) PEG 3350, and 25% PEG 400 before cryocooling in liquid nitrogen.

All diffraction data were collected at 100 K at the Advanced Light Source (Berkeley, CA), beamline 5.0.2. Data were processed and scaled using DENZO and SCALEPACK from the HKL (*24*) program suite (see Table 1). The crystals belong to the *I*23 (*I*-centered cubic) space group ($a = b = c = 165.95$ Å), with one homodimer per asymmetric unit.

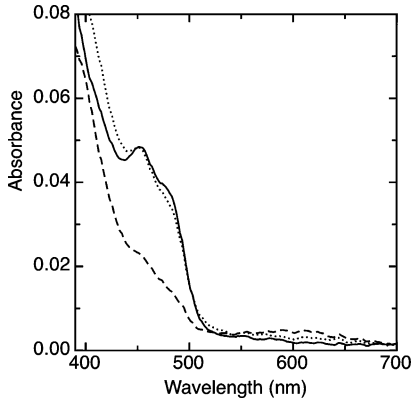

FIGURE 3: Demonstration of *ta*TrxR/Trx reactivity. Reduction of oxidized *ta*TrxR (4 μM) was achieved by use of a modified xanthine/xanthine oxidase system, as described in the Experimental Procedures section. Oxidized *ta*TrxR (solid line) was reduced with xanthine as the source of electrons, over the course of 90 min, in order to build up a stable reduced form of the enzyme (dashed line). Upon introduction of 2 equiv of the *ta*Trx, the sample was completely reoxidized within 1 min (dotted line).

Molecular Replacement Solution and Refinement. The crystal structure of the thioredoxin reductase was solved by the method of molecular replacement. Initial phases were obtained from a full-length polyalanine model of thioredoxin reductase from *Escherichia coli* (PDB code 1TDE) (*25*). The solution was found using PHASER (*26*) with two search models consisting of the flavin binding domain and the NADPH binding domain of the *E. coli* structure, utilizing data from a resolution range of 4.0−12.0 Å. PHASER was first used to find a solution for the FAD binding domain of *ta*TrxR (residues 1−126 and 250−319). This solution was fixed, and a second round of molecular replacement was performed to find the NADPH binding domain (residues 127−249).

Refinement was carried out in CNS (*27*) with rigid body refinement followed by simulated annealing. Manual fitting of amino acid residues was done using XFIT (*28*). Subsequent rounds of refinement included simulated annealing, energy minimization, and *B*-factor refinement without sigma cutoff. Topology and parameter files for the FAD moiety were obtained from HIC-UP (*29*) (PDB code 1N1P). Water molecules were added with CNS and were manually checked against $2F_o - F_c$ and $F_o - F_c$ electron density maps. A composite omit map was prepared in CNS and used to confirm the assignment of model atoms. The final model contains a biologically relevant dimer in the asymmetric unit, which consists of residues 14−319 for molecule A of 319, and residues 13−319 of 319 for molecule B, one flavin molecule per monomer, and 114 water molecules.

RESULTS

Cloning, Purification, and Characterization of taTrxR and taTrx. Using the *T. acidophilum* genome database, we identified two ORFs (Accession nos. Ta0984 and Ta0866): one encoding a putative thioredoxin reductase and the other one encoding a thioredoxin homologue. The Ta0984 gene encodes a protein of 319 amino acids with a predicted molecular mass of 34116 Da (Supporting Information Figure S3). The deduced amino acid sequence contains 28% identity (48% similarity) to the *ec*TrxR (Supporting Information Figure S1). The Ta0866 gene encodes a 133 amino acid protein (Supporting Information Figure S4) with a CxxC disulfide-reducing motif and displays 34% identity (58% similarity) to *ec*Trx (Supporting Information Figure S2). These ORFs have been amplified by PCR, cloned, sequenced, and compared to the sequence in the *T. acidophilum* genome database.

The purified *ta*TrxR yields visible absorption spectra typical for flavoproteins with absorbance maxima at 380 and 460 nm. Freshly purified protein has an A_{280}/A_{460} ratio of between 7.5 and 8.0, in agreement with the full incorporation of FAD as previously observed for *ec*TrxR (*30*). Expression and subsequent purification yield ∼18.5 mg from a 1 L culture. The molecular mass of the protein is estimated to be approximately 34 kDa by SDS−PAGE (Supporting Information Figure S5a). This molecular mass is in agreement with values predicted by the gene analysis. The native molecular mass is determined to be about 70 kDa by gel filtration using a Sephacryl SEC-75 HR 16/60 column. These results suggest that the native state of *ta*TrxR is a homodimer, similar to *ec*TrxR (*31*). Expression of *ta*Trx yields a protein of 13.2 kDa as analyzed by SDS−PAGE (Supporting Information Figure S5b). Subsequent gel filtration using a Sephacryl SEC-30 HR 16/60 column reveals a native molecular mass of ∼13 kDa, suggesting that the *ta*Trx is a monomer in its native state.

Lack of Activity of taTrxR with NADPH or NADH. All previously characterized TrxRs are reduced by NADPH (reviewed in refs (*2, 32*), and (*33*)). For *ec*TrxR, reaction of NADPH with the FAD cofactor occurs rapidly (2000 turnovers FAD^{-1} min^{-1}) with a K_m for NADPH of 1.2 μM (*34*). While there is no measurement of K_m for NADH with *ec*TrxR, it has been estimated to be 400-fold higher than that of NADPH (*31*). Therefore, it is surprising that titration of *ta*TrxR with concentrations of up to 5-fold molar excess of NADPH does not reduce its FAD cofactor to any appreciable extent, showing no significant spectral change in the visible part of the spectra (Figure 2A). For comparison, titration of *ec*TrxR with NADPH results in a rapid reduction of the bound FAD, decreasing the absorbance at 460 nm (Figure 2C). Titration of *ta*TrxR with NADH shows minimal reduction of FAD as indicated by the small change in the shoulder at 460 nm (Figure 2B). Although NADPH is the preferred substrate for *ec*TrxR, NADH does reduce the flavin to some extent in this protein (Figure 2D). The reduction is, in fact, greater than that observed for *ta*TrxR. Compared to the rapid reduction of *ec*TrxR by NADPH (turnover rate is 2000 FAD^{-1} min^{-1}) (*34*), the changes observed for *ta*TrxR appear too slow and too small to be physiologically relevant (Figure 2E). The inability of NADPH or NADH to rapidly reduce *ta*TrxR is not due to instability of these components at 59 °C, the physiological temperature of *T. acidophilum*. Analysis of the time-dependent degradation of NADPH and NADH at 59 °C shows that there is negligible degradation at 5 min under assay conditions, not enough to explain this lack of activity (Supporting Information Figure S6). At the higher temperature of 80 °C, degradation is increased, but even then less than 10% of NADPH or NADH is degraded during the first 5 min of the assay, and only 30% is degraded by 45 min (Supporting Information Figure S6).

Disulfide Reductase Activity of taTrx. The lack of measurable activity between *ta*TrxR and NADPH prevented the use

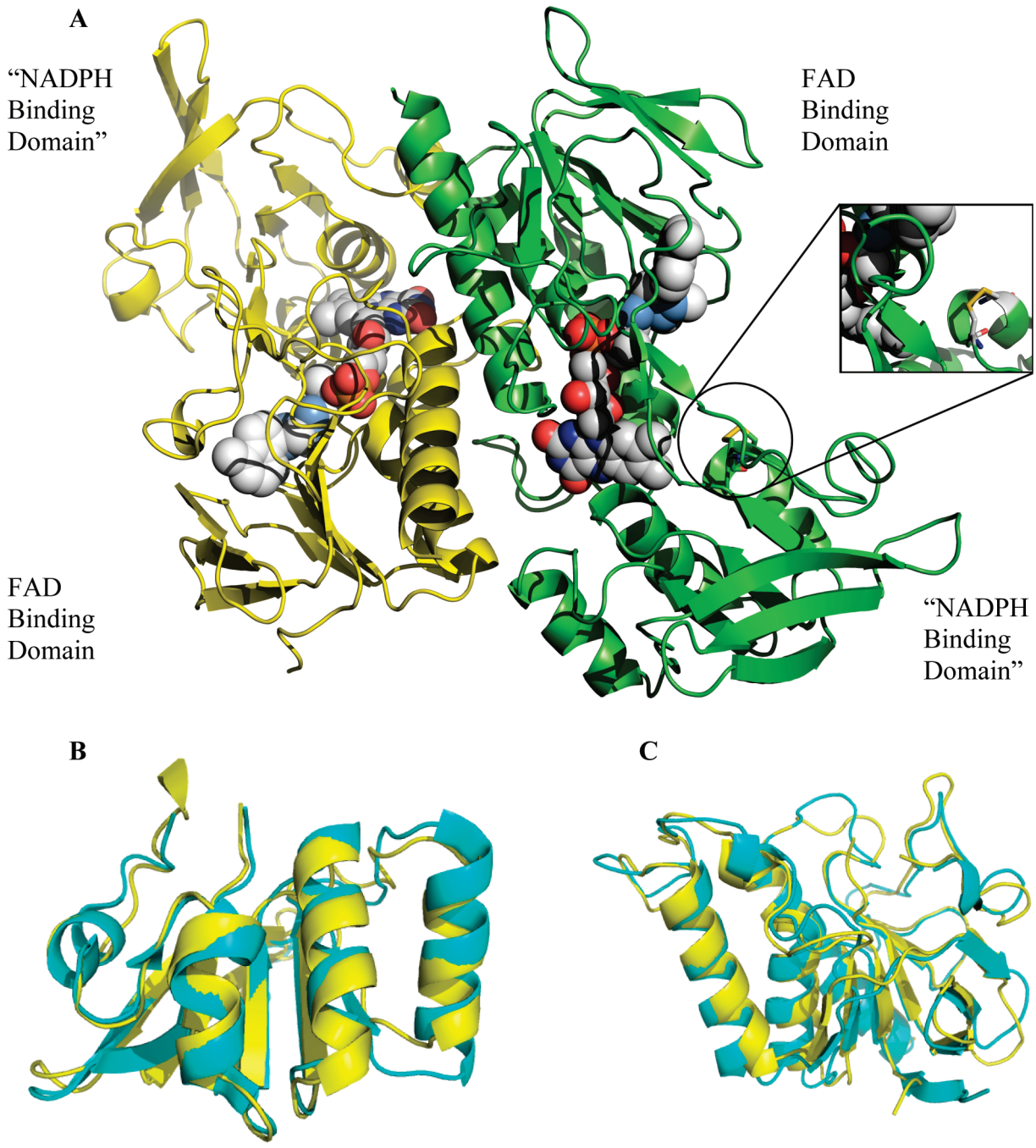

FIGURE 4: Ribbon diagram structure of the *ta*TrxR dimer. (A) Monomers of *ta*TrxR are colored by chain. The flavin molecule (1 per monomer) is represented as space-filled spheres and colored by atom (C in light gray, N in blue, O in red, P in orange). Circle highlights C145/C148 disulfide. (B) Superposition of the *ta*TrxR "NADPH binding domain" with the *ec*TrxR NADPH binding domain. (C) Superposition of the *ta*TrxR FAD binding domain in yellow with the *ec*TrxR FAD binding domain in cyan.

of a coupled assay for *ta*Trx activity, requiring us to turn to other methods to characterize the *ta*Trx. The reduction of insulin disulfides can be monitored by following the increase in turbidity at 650 nm due to the precipitation of the free B-chain (*21*). The recombinant *ta*Trx reduced insulin in a protein concentration-dependent manner (Supporting Information Figure S7). To investigate whether *ta*Trx is able to be reduced by *ec*TrxR, we performed the DTNB assay using NADPH, *ec*TrxR, and *ta*Trx. *ta*Trx is reduced by *ec*TrxR with an apparent K_m of 14.4 (±7.0) μM for the *ec*TrxR (Figure S8). This K_m value is higher than for the *ec*TrxR/*ec*Trx system (K_m of 2.8 μM) (*31*), which is not surprising in that the two proteins (*ec*TrxR and *ta*Trx) did not evolve to interact. These experiments confirm that the *ta*Trx is a thioredoxin-like protein capable of performing disulfide exchange.

Thioredoxin Reductase Activity of taTrxR. To verify that *ta*TrxR can catalyze a disulfide exchange with *ta*Trx, we prereduced *ta*TrxR using a modified xanthine/xanthine oxidase system (see Experimental Procedures) at 25 °C; after complete reduction of the *ta*TrxR flavin, the reduced enzyme was treated with oxidized *ta*Trx. Upon the introduction of 2 equiv of *ta*Trx, the *ta*TrxR was rapidly oxidized, achieving complete reoxidation of the FAD within 1 min (Figure 3). This experiment indicates that *ta*TrxR is a biologically relevant TrxR, which does not use NADPH as a reductant.

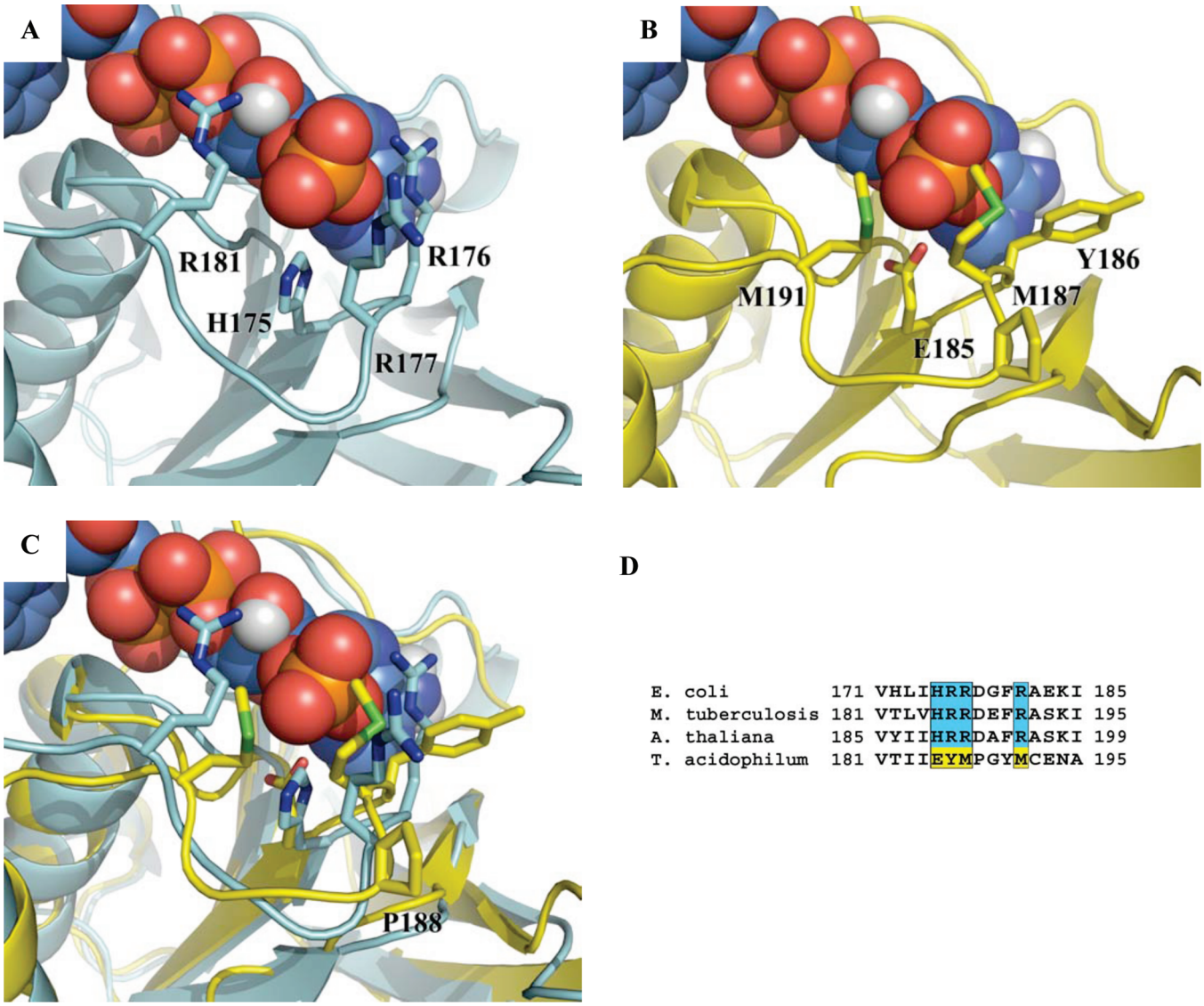

FIGURE 5: Ribbon representation of the *ec*TrxR NADPH binding domain (cyan) (PDB code 1TDF) and *ta*TrxR "NADPH binding domain" (yellow). (A) *ec*TrxR with NADPH binding amino acids, H175, R176, R177, and R181, represented in stick form. (B) *ta*TrxR structure with corresponding structurally aligned amino acids, E185, Y186, M187, and M191, represented in stick form with modeled NADPH. (C) Superposition of *ec*TrxR and *ta*TrxR "NADPH binding domains" with NADPH from the *ec*TrxR structure. (D) Sequence alignment of the "NADPH binding domain" regions.

Overall Structure. The structure of *ta*TrxR was solved to 2.35 Å resolution with the physiological dimer in the asymmetric unit and an R and R_{free} of 22.5% and 26.0%, respectively (see Table 1 for statistics). Each *ta*TrxR monomer consists of a FAD binding domain (residues 14−125 and 251−319) and a "NADPH binding domain" (residues 126−250) (Figure 4A). Each domain of *ta*TrxR is quite similar to the equivalent domain of *ec*TrxR, with an RMSD of 1.23 Å for the 166 Cα of the FAD binding domain and an RMSD of 1.17 Å for 121 Cα of the "NADPH binding domains" (Figure 4B,C). The *ta*TrxR structure has one FAD molecule bound in a similar conformation as the *ec*TrxR structure (Supporting Information Figure S9) and with similar protein−FAD interactions (Supporting Information Figure S10).

*ec*TrxR is known to undergo a large conformational change during catalysis, rotating between a "flavin oxidizing" form (FO) and a "flavin reducing" form (FR) (*25, 35, 36*). In the FR form, the FAD domain is positioned such that NADPH can reduce the FAD by hydride transfer (Figure 4A). In the FO form, the FAD domain is positioned adjacent to the disulfide such that the $FADH_2$ can be oxidized by the disulfide. Structures of both conformations are available for the *E. coli* enzyme: the structure of wild-type *ec*TrxR represents the FO state, and a structure of a complex between *ec*TrxR and *ec*Trx represents the FR state. Interestingly, while all other structures of uncomplexed TrxRs are in the FO state, the *ta*TrxR structure is of the FR form. The *ta*TrxR FR conformation is very similar to that of *ec*TrxR in the FR state with an RMSD of 1.30 Å for chain A and 1.73 Å for chain B when all the Cα atoms are superimposed. As with the *ec*TrxR FR structure, the *ta*TrxR FAD domain is positioned near the putative NADPH binding site and away from the catalytic cysteines (Cys145 and Cys148), which are oxidized with an S−S distance of 2.04 Å. A discussion of the conformational dynamics of TrxRs is available in the accompanying paper (*46*).

Major Differences in the Domain That Typically Binds NADPH. Structural superposition of the "NADPH binding domains" from *ec*TrxR and *ta*TrxR reveals that the

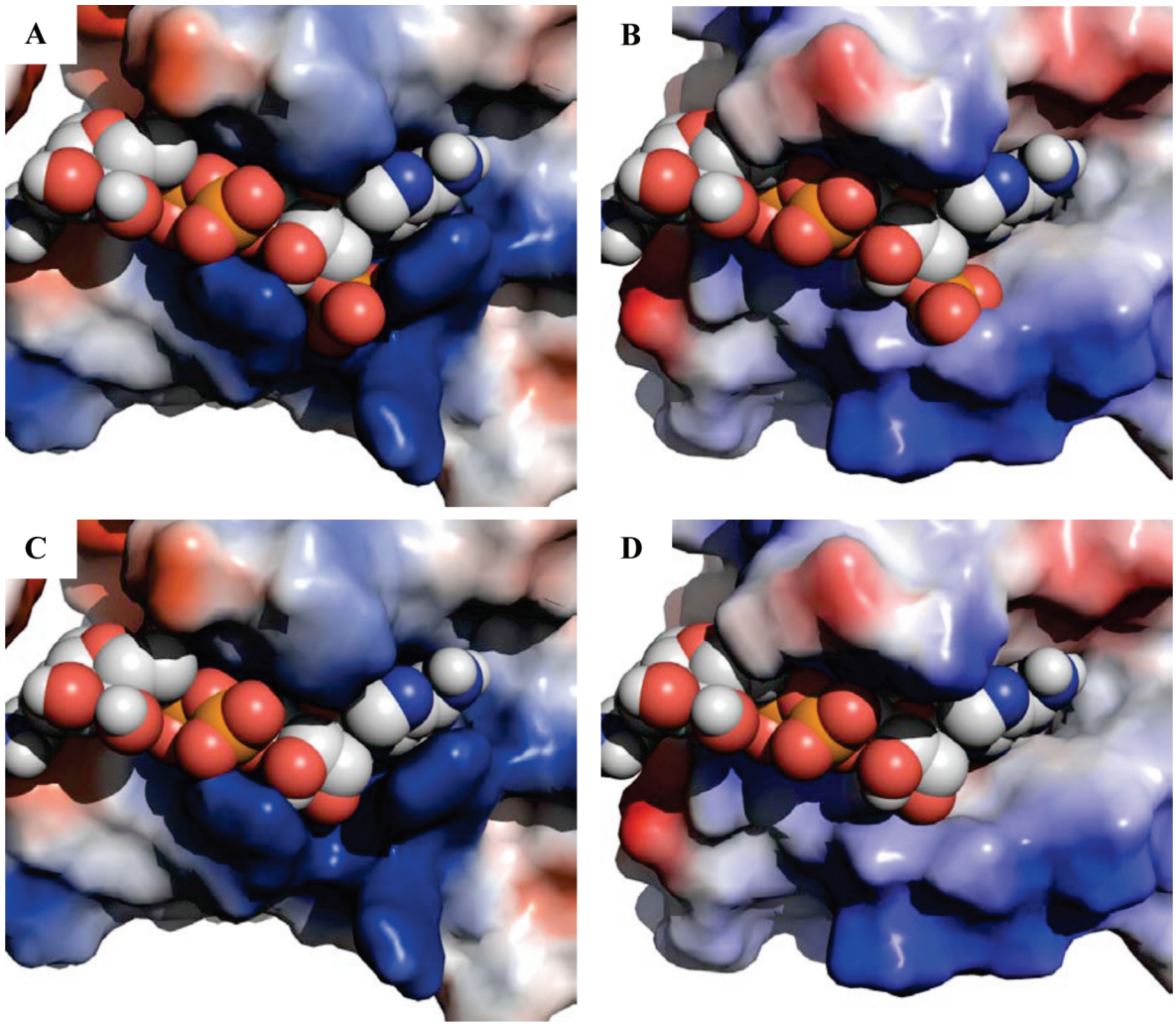

FIGURE 6: Surface representation of NADPH binding pocket with blue representing basic residues; red, acidic residues; and white, neutral residues. (A) *ec*TrxR structure with NADPH bound. (B) *ta*TrxR structure with modeled NADPH. (C) *ec*TrxR structure with NADH modeled in the NADPH binding site. (D) *ta*TrxR structure with NADH modeled in the NADPH binding site. The orientations shown in Figure 6 are similar to those shown in Figure 5, with the panels in Figure 6 rotated slightly to the left so that the NAD(P)H adenine rings are more clearly visible. Surface calculations were made using the APBS module in Pymol (*45*).

backbone of residues 184−191 of the *ta*TrxR structure is constrained into a slightly different conformation than is found in *ec*TrxR. This different loop conformation appears to result from the presence of a proline (P188) in the *ta*TrxR sequence (Figure 5C) and not the presence or absence of nucleotide in the structure (Supporting Information Figure S12). This variation in loop conformation is subtle and is unlikely to explain the lack of affinity of NADPH for the *ta* enzyme. In contrast, while the "NADPH binding domains" for *ta*TrxR and *ec*TrxR display an overall similar fold, close examination reveals several highly conserved residues in all bacterial TrxRs that are not conserved in the *ta*TrxR sequence. The *ec*TrxR structure, which was cocrystallized with $NADP^+$, shows that the NADPH 2′-phosphate is surrounded by a histidine (H175) and three arginines (R176, R177, and R181) creating a positively charged pocket that complements the negatively charged phosphate (Figures 5A, 6A, and S11A). The lower activity (400-fold) for NADH compared to NADPH (*31*) is presumably due to the loss of interactions between the cofactor and residues that form this positively charged pocket (Figure 6C). In *ta*TrxR, none of the residues that form this pocket are conserved. The classic NADPH binding motif VxxxHRRDxxRA is replaced with VxxxEYMPxxMC in *ta*TrxR (Figure 5D). *ec*TrxRs histidine 175, which points directly toward the 2′-phosphate of the NADPH, is substituted with a glutamic acid (E185) in *ta*TrxR, and the three arginine residues (R176, R177, and R181) are replaced by a tyrosine (Y186) and two methionines (M187 and M191) (Figure 5B,C). These substitutions dramatically change the electrostatics of this protein surface (Figures 6 and S11). In a model of NADH bound to *ta*TrxR, an unfavorable interaction between E185 and the 2′-phosphate of NADPH is relieved (Figure 6D), but neither NADPH nor NADH would be expected to bind with any kind of reasonable affinity, consistent with the lack of rapid reduction of FAD by these molecules. Analysis of all known bacterial and archaeal genomes shows that only one other organism, the close cousin to *T. acidophilum*, *Thermoplasma volcanicum*, contains an identical VxxxEYMPxxMC sequence. All others use a variant of the Arg-rich VxxxHRRDxxRA motif.

DISCUSSION

The protein derived from Ta0984 is a thioredoxin reductase. Our structural and biochemical studies reveal a protein

with an FAD cofactor and an overall similar fold to the *ec*TrxR. However, unlike all other characterized TrxRs, *ta*TrxR is not reduced by NADPH. This lack of reactivity is unlikely to be due to redox potential differences between TrxRs (see accompanying paper (*46*)). The redox potential of *ta*TrxR is within 35 mV of *ec*TrxR (−305 vs −270 mV) (*37*), and when reduced with a xanthine/xanthine oxidase system, *ta*TrxR is able to react stoichiometrically with *ta*Trx.

Examination of the *ta*TrxR structure suggests that the lack of activity with NADPH is due to amino acid substitutions as compared to the *E. coli* enzyme. The "NADPH binding site" of *ta*TrxR does not appear to be designed to bind NADPH, with neutral and negatively charged amino acids replacing the canonical Arg-rich motif. The "NADPH binding site" is also structurally constrained by P188. Sequence analysis shows that only one other organism, the closely related *T. volcanicum*, shares *ta*TrxR's unusual sequence.

The lack of a NADPH-dependent TrxR/Trx reduction system in *T. acidophilum* led us to investigate whether this organism might rely heavily on GSSGR/Grx systems instead of on thioredoxins. Analysis of the *T. acidophilum* genome, however, revealed no GSSGR/Grx system, nor enzymes for the biosynthesis of glutaredoxin (*38*). Our extensive data mining and sequence alignments have not produced any near or distantly related GSSGR/Grx proteins from this organism.

We also considered whether *T. acidophilum* uses NADH or NADPH in other cellular processes. Our genomic analysis reveals a putative NAD kinase, the enzyme responsible for the conversion of NAD to NADP, and several putative NADH and NADPH utilizing enzymes, which suggests that *T. acidophilium* does use these cofactors. To date, there are only a few characterized enzymes in *T. acidophilum* that use NADH (aldohexose dehydrogenase) (*39*) or NADPH (glyderaldehyde dehydrogenase) (*40*) or both NADH and NADPH as substrates (*41*). However, the use of NADPH or NADH by any *T. acidophilum* enzyme, in addition to the presence of the NAD kinase gene, indicates that availability of these cofactors is not the reason for the observed variation in the TrxR protein.

The above data challenges the paradigm shown in Figure 1A. Our data block the arrow to the left, and the lack of GSSGR/Grx blocks the arrow to the right. Given this, we revisited the *T. acidophilum* genome to search again for other putative TrxR sequences and found none. Unless there is a TrxR with a very different sequence, we have cloned the only one in *T. acidophilum*.

If NADPH does not reduce this *ta*TrxR, and this TrxR is the only TrxR in *T. acidophilum*, and there are no obvious GSSGR/Grx candidates, there must be some small molecule that can provide reducing equivalents or the cytoplasmic environment would quickly oxidize and the organism would expire. One such molecule, coenzyme F420, has been shown to be a physiological reductant in methane-reducing thermophilic organisms (reviewed in refs *42*−*44*). However, genomic analysis of *T. acidophilum* does not reveal any of the enzymes involved in the biosynthesis of F420. The lack of molecular pathways for the biosynthesis of coenzyme F420, along with the lack of other F420-dependent enzymes in *T. acidophilum*, seems to indicate that coenzyme F420 is not a reductant of *ta*TrxR. Of course, we cannot rule out the possibility that F420 is generated by a different set of enzymes in this organism.

CONCLUSIONS

To date, there is no well-characterized example of an organism that uses a reductant other than NADPH to maintain its intracellular redox environment. Here we present evidence that one organism, *T. acidophilum*, which does not contain a Grx system, uses an alternative method to reduce the bound FAD of the TrxR system. This work lays the foundation for a biochemical search for the molecular redox partners of *T. acidophilum* TrxR.

ACKNOWLEDGMENT

The authors thank Dr. Scott Mulrooney and Prof. Charles Williams, Jr., for the generous donation of the *ec*TrxR overexpression system. Portions of this research were carried out at the Stanford Synchrotron Radiation Laboratory, a national user facility operated by Stanford University on behalf of the U.S. Department of Energy, Office of Basic Energy Sciences. The SSRL Structural Molecular Biology Program is supported by the Department of Energy, Office of Biological and Environmental Research, and by the National Institutes of Health, National Center for Research Resources, Biomedical Technology Program, and the National Institute of General Medical Sciences.

SUPPORTING INFORMATION AVAILABLE

Sequence alignments of TrxRs and Trxs, sequences of *ta*TrxR and *ta*Trx, a figure showing gel analysis of purified protein, figures showing the temperature-dependent degradation of NADH and NADPH, results of insulin assays, results of *ta*Trx and *ec*TrxR reduction of DTNB, a figure of FAD in composite omit map density, schematic representation interactions between FAD and *ta*TrxR, and structural comparison figures. This material is available free of charge via the Internet at http://pubs.acs.org.

REFERENCES

1. Jaeger, T., and Flohe, L. (2006) The thiol-based redox networks of pathogens: unexploited targets in the search for new drugs. *Biofactors 27*, 109–120.
2. Arner, E. S., and Holmgren, A. (2000) Physiological functions of thioredoxin and thioredoxin reductase. *Eur. J. Biochem. 267*, 6102–6109.
3. Masutani, H., Ueda, S., and Yodoi, J. (2005) The thioredoxin system in retroviral infection and apoptosis. *Cell Death Differ. 12* (Suppl. 1), 991–998.
4. Gromer, S., Urig, S., and Becker, K. (2004) The thioredoxin system—from science to clinic. *Med. Res. Rev. 24*, 40–89.
5. Mustacich, D., and Powis, G. (2000) Thioredoxin reductase. *Biochem. J. 346*, 1–8.
6. Stroher, E., and Dietz, K. J. (2006) Concepts and approaches towards understanding the cellular redox proteome. *Plant Biol. (Stuttgart) 8*, 407–418.
7. Toledano, M. B., Kumar, C., Le Moan, N., Spector, D., and Tacnet, F. (2007) The system biology of thiol redox system in Escherichia coli and yeast: differential functions in oxidative stress, iron metabolism and DNA synthesis. *FEBS Lett. 581*, 3598–3607.
8. Herrick, J., and Sclavi, B. (2007) Ribonucleotide reductase and the regulation of DNA replication: an old story and an ancient heritage. *Mol. Microbiol. 63*, 22–34.
9. Nordlund, P., and Reichard, P. (2006) Ribonucleotide reductases. *Annu. Rev. Biochem. 75*, 681–706.

10. Shao, J., Zhou, B., Chu, B., and Yen, Y. (2006) Ribonucleotide reductase inhibitors and future drug design. *Curr. Cancer Drug Targets 6*, 409–431.
11. Hashemy, S. I., Ungerstedt, J. S., Zahedi Avval, F., and Holmgren, A. (2006) Motexafin gadolinium, a tumor-selective drug targeting thioredoxin reductase and ribonucleotide reductase. *J. Biol. Chem. 281*, 10691–10697.
12. Urig, S., and Becker, K. (2006) On the potential of thioredoxin reductase inhibitors for cancer therapy. *Semin. Cancer Biol. 16*, 452–465.
13. Becker, K., Gromer, S., Schirmer, R. H., and Muller, S. (2000) Thioredoxin reductase as a pathophysiological factor and drug target. *Eur. J. Biochem. 267*, 6118–6125.
14. Darland, G., Brock, T. D., Samsonoff, W., and Conti, S. F. (1970) A thermophilic, acidophilic mycoplasma isolated from a coal refuse pile. *Science 170*, 1416–1418.
15. Searcy, D. G. (1976) Thermoplasma acidophilum: intracellular pH and potassium concentration. *Biochim. Biophys. Acta 451*, 278–286.
16. Hsung, J. C., and Haug, A. (1975) Intracellular pH of Thermoplasma acidophila. *Biochim. Biophys. Acta 389*, 477–482.
17. Ruepp, A., Graml, W., Santos-Martinez, M. L., Koretke, K. K., Volker, C., Mewes, H. W., Frishman, D., Stocker, S., Lupas, A. N., and Baumeister, W. (2000) The genome sequence of the thermoacidophilic scavenger Thermoplasma acidophilum. *Nature 407*, 508–513.
18. Altschul, S. F., Madden, T. L., Schaffer, A. A., Zhang, J., Zhang, Z., Miller, W., and Lipman, D. J. (1997) Gapped BLAST and PSI-BLAST: a new generation of protein database search programs. *Nucleic Acids Res. 25*, 3389–3402.
19. Higgins, D. T. J., Gibson, T., Thompson, J. D., Higgins, D. G., and Gibson, T. J. (1994) CLUSTAL W: improving the sensitivity of progressivemultiple sequence alignment through sequence weighting,position-specific gap penalties and weight matrix choice. *Nucleic Acids Res.* 4673–4680.
20. Gouet, P., Courcelle, E., Stuart, D. I., and Metoz, F. (1999) ESPript: analysis of multiple sequence alignments in PostScript. *Bioinformatics 15*, 305–308.
21. Holmgren, A. (1979) Thioredoxin catalyzes the reduction of insulin disulfides by dithiothreitol and dihydrolipoamide. *J. Biol. Chem. 254*, 9627–9632.
22. Arner, E. S., Zhong, L., and Holmgren, A. (1999) Preparation and assay of mammalian thioredoxin and thioredoxin reductase. *Methods Enzymol. 300*, 226–239.
23. Massey, V., Brumby, P. E., and Komai, H. (1969) Studies on milk xanthine oxidase. Some spectral and kinetic properties. *J. Biol. Chem. 244*, 1682–1691.
24. Otwinowski, Z., and Minor, W. (1997) Processing of X-ray diffraction data collected in oscillation mode. *Methods Enzymol. 276*, 307–326.
25. Waksman, G., Krishna, T. S., Williams, C. H., Jr., and Kuriyan, J. (1994) Crystal structure of Escherichia coli thioredoxin reductase refined at 2 Å resolution. Implications for a large conformational change during catalysis. *J. Mol. Biol. 236*, 800–816.
26. McCoy, A. J., Grosse-Kunstleve, R. W., Storoni, L. C., and Read, R. J. (2005) Likelihood-enhanced fast translation functions. *Acta Crystallogr., Sect. D: Biol. Crystallogr. 61* (Part 4), 458–464.
27. Brunger, A. T., Adams, P. D., Clore, G. M., DeLano, W. L., Gros, P., Grosse-Kunstleve, R. W., Jiang, J. S., Kuszewski, J., Nilges, M., Pannu, N. S., Read, R. J., Rice, L. M., Simonson, T., and Warren, G. L. (1998) Crystallography & NMR system: A new software suite for macromolecular structure determination. *Acta Crystallogr., Sect. D: Biol. Crystallogr. 54* (Part 5), 905–921.
28. McRee, D. E. (1999) XtalView/Xfit—A versatile program for manipulating atomic coordinates and electron density. *J. Struct. Biol. 125*, 156–165.
29. Kleywegt, G. J., and Jones, T. A. (1998) Databases in protein crystallography. *Acta Crystallogr., Sect. D: Biol. Crystallogr. 54* (Part 6, Part 1), 1119–1131.
30. Williams, C. H., Jr., Zanetti, G., Arscott, L. D., and McAllister, J. K. (1967) Lipoamide dehydrogenase, glutathione reductase, thioredoxin reductase, and thioredoxin. *J. Biol. Chem. 242*, 5226–5231.
31. Thelander, L. (1967) Thioredoxin reductase. Characterization of a homogenous preparation from Escherichia coli B. *J. Biol. Chem. 242*, 852–859.
32. Williams, C. H., Arscott, L. D., Muller, S., Lennon, B. W., Ludwig, M. L., Wang, P. F., Veine, D. M., Becker, K., and Schirmer, R. H. (2000) Thioredoxin reductase two modes of catalysis have evolved. *Eur. J. Biochem. 267*, 6110–6117.
33. Biaglow, J. E., and Miller, R. A. (2005) The thioredoxin reductase/thioredoxin system: novel redox targets for cancer therapy. *Cancer Biol. Ther. 4*, 6–13.
34. Williams, C. H., Jr. (1976) Flavin-Containing Dehydrogenases, in *The Enzymes* (Boyer, P. D., Ed.) 3rd ed., Vol. 1, pp 89−173, Academic Press, New York.
35. Lennon, B. W., Williams, C. H., Jr., and Ludwig, M. L. (1999) Crystal structure of reduced thioredoxin reductase from Escherichia coli: structural flexibility in the isoalloxazine ring of the flavin adenine dinucleotide cofactor. *Protein Sci. 8*, 2366–2379.
36. Wang, P. F., Veine, D. M., Ahn, S. H., and Williams, C. H., Jr. (1996) A stable mixed disulfide between thioredoxin reductase and its substrate, thioredoxin: preparation and characterization. *Biochemistry 35*, 4812–4819.
37. O'Donnell, M. E., and Williams, C. H., Jr. (1983) Proton stoichiometry in the reduction of the FAD and disulfide of Escherichia coli thioredoxin reductase. Evidence for a base at the active site. *J. Biol. Chem. 258*, 13795–13805.
38. Copley, S. D., and Dhillon, J. K. (2002) Lateral gene transfer and parallel evolution in the history of glutathione biosynthesis genes. *Genome Biol. 3*, 1–16.
39. Reher, M., and Schonheit, P. (2006) Glyceraldehyde dehydrogenases from the thermoacidophilic euryarchaeota Picrophilus torridus and Thermoplasma acidophilum, key enzymes of the non-phosphorylative Entner-Doudoroff pathway, constitute a novel enzyme family within the aldehyde dehydrogenase superfamily. *FEBS Lett. 580*, 1198–1204.
40. Nishiya, Y., Tamura, N., and Tamura, T. (2004) Analysis of bacterial glucose dehydrogenase homologs from thermoacidophilic archaeon Thermoplasma acidophilum: finding and characterization of aldohexose dehydrogenase. *Biosci., Biotechnol., Biochem. 68*, 2451–2456.
41. Smith, L. D., Budgen, N., Bungard, S. J., Danson, M. J., and Hough, D. W. (1989) Purification and characterization of glucose dehydrogenase from the thermoacidophilic archaebacterium Thermoplasma acidophilum. *Biochem. J. 261*, 973–977.
42. Fischer, M., and Bacher, A. (2005) Biosynthesis of flavocoenzymes. *Nat. Prod. Rep. 22*, 324–350.
43. Graupner, M., Xu, H., and White, R. H. (2002) The pyrimidine nucleotide reductase step in riboflavin and F(420) biosynthesis in archaea proceeds by the eukaryotic route to riboflavin. *J. Bacteriol. 184*, 1952–1957.
44. Mack, M., and Grill, S. (2006) Riboflavin analogs and inhibitors of riboflavin biosynthesis. *Appl. Microbiol. Biotechnol. 71*, 265–275.
45. Baker, N. A., Sept, D., Joseph, S., Holst, M. J., and McCammon, J. A. (2001) Electrostatics of nanosystems: application to microtubules and the ribosome. *Proc. Natl. Acad. Sci. U.S.A. 98*, 10037–10041.
46. Hamill, M. J., Chobot, S. E., Hernandez, H. H., Drennan, C. L., and Elliott, S. J. (2008) Direct electrochemical analyses of a thermophilic thioredoxin reductase: Interplay between conformational change and redox chemistry. *Biochemistry 47*, 9738–9746.

BI8006753